$C_{61}H_2$ in Molecular and Solid Phases: Density-Functional Approach to Structural and Electronic Properties

Alessandro Curioni,[†,‡] Paolo Giannozzi,[†,‡] Jürg Hutter,[†] and Wanda Andreoni*[,†]

IBM Research Division, Zurich Research Laboratory, CH-8803 Rüschlikon, Switzerland, and Scuola Normale Superiore, piazza dei Cavalieri 7, I-56126 Pisa, Italy

Received: September 21, 1994; In Final Form: December 7, 1994[⊗]

The two low-energy isomers of $C_{61}H_2$ are the parent molecules of fulleroids and methanofullerenes. We present a thorough study of their structural and electronic properties within the density functional theory, in the local-density approximation and also including gradient corrections to the exchange and correlation functionals. Calculations are performed both on the isolated molecules and on the solid phases. Changes with respect to C_{60} as well as differences between the two $C_{61}H_2$ isomers are described with regard to geometrical characteristics, bond patterns, valence charge distribution, and electronic energy bands. Our results can be considered a paradigm for the study of fulleroids and methanofullerenes.

I. Introduction

In contrast to earlier expectations, the superalkane nature of C_{60} has been firmly established[1] and with it its ready response to chemical additions, which has opened the way to its functionalization (see, e.g., refs 2−5). In fact, several methods to functionalize C_{60} have been attempted, and a number of different new molecules have thus been obtained. Especially interesting are the so-called fulleroid (or homofullerene) and methanofullerene families,[4,6] which retain the desired chemical properties of the fullerenes in spite of local modifications of the geometrical skeleton. The parent molecules are the two isomers of $C_{61}H_2$. Both of them have been isolated and uniquely characterized with nuclear magnetic resonance (NMR) spectroscopy.[7,8] NMR data and subsequent empirical calculations, in fact, were sufficient to establish the distinctive structural features. In the methanofullerene isomer (generally called the 6,6-cyclopropane isomer), the methylene carbon bridges one of the (30) double bonds of C_{60}, which remains "closed", thus giving rise to a cyclopropane-like local structure. The two hydrogens are equivalent, so proton NMR yields only one signal. In the fulleroid or homofullerene isomer (called the 5,6-annulene isomer), the methylene carbon bridges one of the (60) single bonds, which opens and gives rise to an annulene-like arrangement. In this case the two hydrogens are not equivalent, so two resonance lines are detected with proton NMR measurements.

Solid $C_{61}H_2$ has so far been characterized only for the 5,6-isomer.[9] Powder X-ray diffraction shows that, in analogy with C_{60} but at a higher temperature (290 instead of 260 K), the 5,6-isomer undergoes a disorder−order transition from a face-centered-cubic structure with orientationally disordered molecules (space group $Fm\bar{3}$) to a simple cubic modification with four orientationally ordered molecules per unit cell ($Pa\bar{3}$ space group).[9] Quasielastic neutron scattering and NMR have been used to study the molecular dynamic in the solid state.[10]

Little is known about the electronic properties of $C_{61}H_2$. The ultraviolet absorption spectrum of the 5,6-isomer is reported to be "virtually identical" to that of C_{60}.[7] The 6,6-isomer also has a very similar UV spectrum with, however, a new feature at about 430 nm, which seems to be characteristic of 6,6-bridged methanofullerenes.[8,11] Photoemission spectra are unavailable, owing to the impossibility of preparing films on account of the low thermal stability of the molecules.[9] Also, alkali-metal intercalation has reduced thermal activity relative to C_{60} and C_{70}. Attempts thus far have yielded only mixed-phase product with no sign of superconductivity. The strategies of "chimie douce" may be more rewarding.[12]

Theoretical approaches have so far been restricted to the study of the molecules and focused on calculating the energetics of the two isomers. All calculations agree in predicting an "opening" transannular bond for the 5,6-isomer and a "closed" one for the 6,6-isomer: a result that can be anticipated on the basis of the conjugation properties of the molecules.[4] However, concerning the energy preference for one or the other configuration, semiempirical calculations yield contrasting results.[13] Instead, first-principle all-electron calculations, within the density functional theory (DFT) scheme as well as at the Hartree−Fock level, consistently predict the 6,6-isomer to be the ground-state structure by an albeit small energy difference of a few kilocalories per mole.[14] No report exists, so far, describing calculations of the electronic properties of these molecules.

In this paper, we present an investigation of the structural and electronic properties of the two isomers in the molecular form as well as in solid phases. In the latter, the molecules are assumed to be orientationally ordered and to have their centers at the corners of a face-centered-cubic lattice. This allows us to identify the salient solid-state effects as well as the main differences from C_{60}. For this we use the Car-Parrinello method,[15] which has already been successfully applied to a number of fullerenes and fullerene-based materials.[16] The basic approach to the electronic structure is the density functional theory within the pseudopotential formalism. We use it at three different levels of approximation of the energy functional:[17] the local-density approximation (LDA) and including gradient corrections to the exchange functional only (GCX) as well as to both exchange and correlation functionals (GCXC). To optimize the electronic variables, we use the recently implemented[18] direct inversion in iterative subspace (DIIS) method.[19] To optimize the geometrical variables, we adopt a combined DIIS quasi-Newton method (with an empirical initial Hessian).[20] In section II we provide some computational details and test the accuracy of the calculations. In sections III and IV, we discuss our results concerning the structural and the electronic

[†] Zurich Research Laboratory.
[‡] Scuola Normale Superiore.
[⊗] Abstract published in *Advance ACS Abstracts,* February 15, 1995.

0022-3654/95/2099-4008$09.00/0

TABLE 1: C_{60} Interatomic Distances (in Å) Calculated in LDA (Two Different Energy Cutoffs), GCX, and GCXC[a]

approximation	double bond	single bond
p-LDA (35 Ry)	1.390	1.447
p-LDA (55 Ry)	1.391	1.444
p-GCX (55 Ry)	1.402	1.460
p-GCXC (55 Ry)	1.400	1.454
experiment (NMR[26])	1.40 ± 0.015	1.45 ± 0.015

[a] p denotes the pseudopotential approximation.

properties of the two isomers in the molecular and solid phases, respectively. Conclusions are drawn in section V.

II. Computational Framework and Convergence Tests

Our calculations are based on the DFT approach to the electronic structure problem. In the LDA, we use the Perdew–Zunger parametrization[21] for the correlation energy functional. For the gradient corrections to the LDA exchange and correlation energy functionals, we adopt the parametrization schemes suggested by Becke[22] and Perdew,[23] respectively. The 1s core electrons of carbon are considered frozen, and their effects on the valence electrons are modeled by atomic angular-momentum-dependent and norm-conserving pseudopotentials. Hydrogen is treated with a local pseudopotential. The LDA pseudopotentials are from ref 24. The GCX and GCXC pseudopotentials have been generated with the procedure introduced by Troullier and Martins.[25] The pseudowavefunctions are expanded into plane waves. We have checked the convergence of the calculations in terms of the energy cutoff of this expansion. While the main and relevant features of the electronic structure are quite insensitive, sizable changes occur in some of the structural parameters, namely, the interatomic distances close to the methylene group. This test is shown in Table 1, which lists results for the two isomers and for C_{60}. Here, we also compare the LDA structural parameters with those calculated in the GCX and in the GCXC. As is quite common, gradient corrections result in an overall increase of the interatomic distances. In C_{60}, however, this amounts to an increase of the radius of at most 1% [3.53 Å (LDA), 3.57 Å (GCX), and 3.55 Å (GCXC)]. In particular, the difference between the two bond lengths retains a value of 0.05–0.06 Å, which agrees well with experiment.[26] It is also worth noting that results for molecular structural parameters obtained with the gradient-corrected functionals are not necessarily better than those obtained with LDA.[27,28]

Calculations of the solids are performed in the LDA scheme, using only the Γ-point as representative of the irreducible Brillouin zone. In the case of solid C_{60}, this approximation is poor for the determination of the bulk modulus[29] and of the structural changes induced by alkali-metal intercalation.[30] However, it is sufficiently accurate for the determination both of the solid-state effects on the molecular structure and of the electron energy bands.

III. Molecules: Comparison of the Two Isomers

Bridging a double or a single bond with a CH_2 group implies substantially different modifications of the structure and of the electronic properties of C_{60}. For both cases we shall calculate the deformations induced on the fullerene skeleton and on the bond network as well as on the HOMO's and the LUMO's. As far as structure and energetics are concerned, we shall discuss the results obtained with LDA and with Becke–Perdew gradient corrections. Those derived with GCX are only reported for sake of comparison and completeness. The discussion on the electronic properties will mainly refer to the LDA results. As we have verified, these are highly independent of the approximation used for the exchange and correlation functionals.

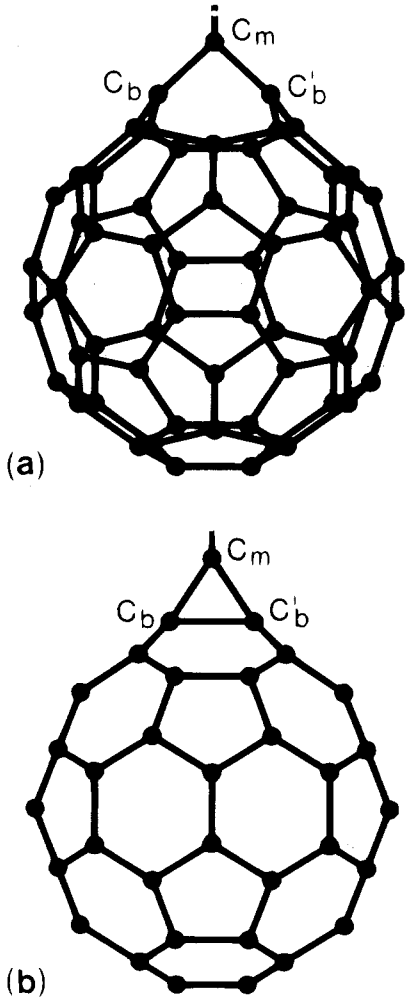

Figure 1. $C_{61}H_2$: Structure of (a) the 5,6-annulene and (b) the 6,6-cyclopropane isomers.

A. Structure and Energetics. Figure 1 shows the geometry of the two isomers: (a) the 5,6-annulene isomer (C_s symmetry; henceforth denoted "A") and (b) the 6,6-cyclopropane isomer (C_{2v} symmetry; henceforth denoted "B"). Tables 2 and 3 contain their geometrical characteristics around the CH_2 group. In agreement with previous *ab initio* calculations,[14] isomer A corresponds to the breaking of the single bond, while in B the double bond loses its character and elongates by more than 0.2 Å. The value calculated at equilibrium for these distances at the bridge changes only by 1–2%, depending on the approximation used for the exchange and correlation functionals. Still, this is the parameter which we find most sensitive to the approximation. In this range of variation (~0.02 Å around the optimized value), the energy is, however, extremely flat.

Note that the values for the interatomic distances at the bridge calculated in ref 14 at the local-spin-density (LSD-DZP) level are in very good agreement with our converged LDA values. Unfortunately, no other structural information is given in ref 14, so we cannot draw further comparisons.

The methylene carbon lies at a similar distance from the center of the 60-atom cage in the two isomers but sticks out ~0.2 Å more in B (in LDA the radius is 4.71 Å in A and 4.93 Å in B; in GCXC it is 4.78 and 4.94 Å, respectively). The new carbon–carbon bonds correspond to close values of the bond lengths in A and B but are ~0.05 Å shorter than that of the single bonds of fourfold tetrahedrally coordinated carbons

TABLE 2: $C_{61}H_2$, 5,6-Isomer. Interatomic Distances (in Å) and Bond Angles (in Degrees) Calculated in LDA (Two Different Energy Cutoffs), GCX, and GCXC[a]

approximation	$d(C_b-C_{b'})$	$d(C_b-C_m)$	$d(C_m-H)$	$\alpha(\angle C_bC_mC_{b'})$	$\alpha(\angle HC_mH)$	$\alpha(\angle HC_mC)$	av db	av sb
p-LDA (35 Ry)	2.170	1.486	1.104	94	111	113	1.392	1.450
p-LDA (55 Ry)	2.142	1.468	1.101	94	111	113	1.388	1.438
p-GCX (55 Ry)	2.218	1.499	1.090	95	110	113	1.403	1.460
p-GCXC (55 Ry)	2.186	1.488	1.097	94	110	113	1.400	1.456
LSD-DZP[14]	2.16							

[a] p denotes the pseudopotential approximation.

TABLE 3: $C_{61}H_2$, 6,6-Isomer. Interatomic Distances (in Å) and Bond Angles (in Degrees) Calculated in LDA (Two Different Energy Cutoffs), GCX, and GCXC[a]

approximation	$d(C_b-C_{b'})$	$d(C_b-C_m)$	$d(C_m-H)$	$\alpha(C_bC_mC_{b'})$	$\alpha(HC_mH)$	$\alpha(HC_mC)$	av db	av sb
p-LDA (35 Ry)	1.646	1.494	1.100	67	115	116	1.390	1.450
p-LDA (55 Ry)	1.616	1.477	1.096	66	115	117	1.387	1.438
p-GCX (55 Ry)	1.682	1.504	1.085	68	117	117	1.402	1.461
p-GCXC (55 Ry)	1.670	1.497	1.092	68	115	116	1.400	1.456
LSD-DZP[14]	1.62							

[a] p denotes the pseudopotential approximation.

(1.54 Å). The bond angles with the bridging carbon are, however, very different in the two cases, with a strong angle strain in B, typical of the bent bonds of cyclopropanes. In A, breaking of the pentagon–hexagon transannular bond and addition of two new C–C bonds results in the formation of two 3D bond rings about the methylene carbon: a distorted heptagon with angles in the range 94–125° and a distorted hexagon with angles in the range 94–117°. In B, the two adjacent heptagonal rings have angles in the range 67–124°. The average values of the two characteristic bond lengths calculated on the 89 fullerene bonds (Tables 2 and 3) do not vary appreciably in either case. The changes Δl of all 89 bonds (single and double) with respect to the C_{60} molecule are plotted in Figure 2 as a function of the distance of the center of the individual bond from the methylene carbon atom C_m for the GCXC geometries. We found that, although the precise values change on passing from the LDA to the GCXC models, in both cases the sizable part of the structural relaxation is spatially rather confined. In A the deformation involves indeed a larger portion of the molecule, because the perturbation extends at least 1 Å farther from C_m. However, the two on-cage bonds of the two bridge atoms are rigid (bond lengths and angles remain largely unchanged) in A, while in B they elongate by ~0.03 Å and the angles shrink by 5° as a result of the redistribution of the angle strain.

In conclusion, the rearrangement of the fullerene structure in the two isomers reveals that isomer B is more similar to C_{60}, but the annulene-like configuration in A is more favorable for the CH_2 addition. This is especially clear from a quick examination of the energetics. The distortion of the bulky fullerene corresponds to a much higher cost in A than in B (in LDA ~3.4 vs ~1.5 eV; in GCXC: ~3.0 vs ~1.3 eV). However, the total energy difference ΔE of the two $C_{61}H_2$ isomers, although still favoring isomer B, is 1 order of magnitude smaller (see Table 4). Indeed, the values calculated for ΔE are at the limit of accuracy of the calculations: from ~0.2 eV (4.5 kcal/mol) in LDA, it reduces to ~0.1 eV (2.3 kcal/mol) in GCXC. This tendency was also found in ref 14 (see Table 4), where, however, the geometry was not relaxed at the NLSD level and the energy change with respect to LSD was calculated perturbatively. We have found that for fixed LDA geometry, the GCXC value for ΔE is indeed very close to the final one (0.08 vs 0.10 eV).

In A the two hydrogens are inequivalent, but the C–H distances differ only by 0.002 Å and the ∠HCH angles by less than 0.1°, i.e., by amounts smaller than the accuracy itself. The

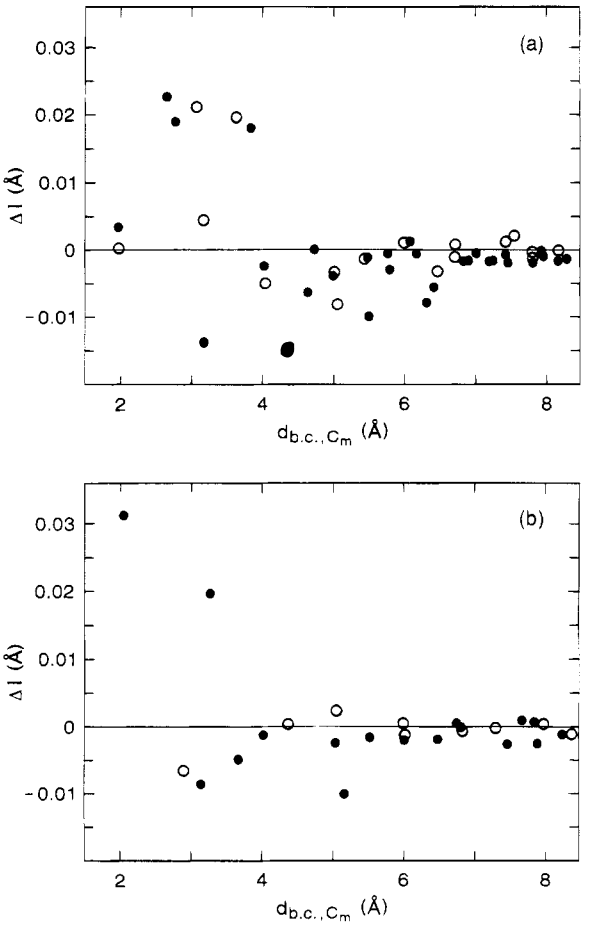

Figure 2. $C_{61}H_2$: Change of the 89 bond lengths on the C_{60}-like portion of the molecule with respect to C_{60} as a function of the distance of the bond center from C_m. Parts a and b refer to isomers A and B, respectively, using the GCXC optimized structures. Empty and filled circles refer to the single and double bonds of C_{60}, respectively.

∠HC_mH angle in B is very close to that measured in cyclopropane (115.85).[31] The decrease of this angle on passing from isomer B to A is consistent with the behavior calculated in cyclopropane upon the opening of one C–C bond.[32]

B. Electronic Properties. Parts a and b of Figure 3 illustrate two iso-electron density surfaces in the environment of the CH_2 group in isomers A and B, respectively. While in A the lack of charge between the two nonbonded bridge atoms is apparent, there still is a residual density in B, indicating the presence of

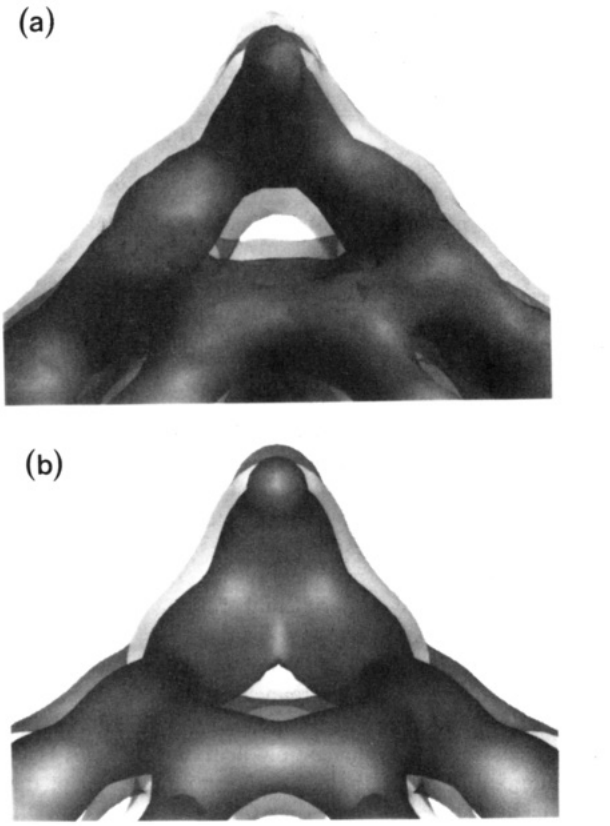

Figure 3. $C_{61}H_2$: Electron density distribution in (a) the 5,6 and (b) the 6,6-isomers. The two surfaces illustrated are 0.10 (lighter) and 0.17 (darker) e/(a.u.)^3.

TABLE 4: $C_{61}H_2$. Energy Difference (in eV) between the Two Isomers Calculated in Different Approximations (See Text), $\Delta E = E_{(5,6)} - E_{(6,6)}$

p-LDA (35 Ry)	p-LDA (55 Ry)	LSD-DZP[14]	p-GCX (55 Ry)	p-GCXC (55 Ry)	NLSD-DZP[14]
0.200	0.193	0.195	−0.015	0.097	0.108

a weak bond between them. The bent bonds between the fullerene atoms and the methylene carbon, characteristic of cyclopropane, are also clearly visible in B.

In order to obtain a more detailed description of the charge distribution, we integrate it on Voronoy polyhedra[33] centered around each atom, performing this calculation both on the $C_{61}H_2$ molecule and on the deformed C_{60} cage alone. We denote the integrated charges by Q_v and $Q_{v,d}$, respectively. In Figure 4 we plot $Q_v - 4$ and the difference $\Delta Q_v = Q_v - Q_{v,d}$ for all the atoms on the bulky fullerene as a function of the distance from the top carbon atom C_m. The comparison allows us to distinguish the effects due to the structural changes from those due to the addition. In both cases, the charge inhomogeneity ($Q_v - 4$) is mainly confined to the close environment of the CH_2 group. At the level of the bridge atoms, the structural change is dominant and causes depletion in both cases, which is stronger in isomer A, owing to the breaking of the bond between the bridge atoms. The second feature in Figure 4 refers to the other atoms that are bonded to those at the bridge. In A, the structural change by itself would redistribute the change in favor of these atoms, but the addition depopulates them. In B, both processes tend to depopulate them. As a net result, the CH_2 group gains 0.9e in A and 0.6e in B. ΔQ_v decays rapidly with distance, indicating that all "long-range" variations in Q_v are due to structural effects only.

Figure 5a,b illustrates the density of the occupied electron states (EDOS) in the two isomers compared to that of C_{60}, with an empirical broadening of the levels. A comparison between them is shown in Figure 5c. The effect of symmetry lowering

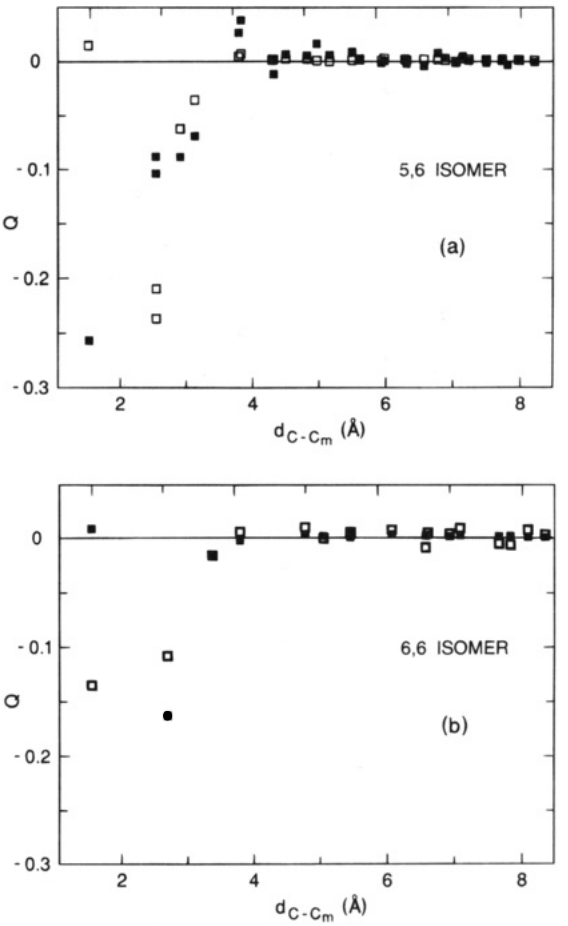

Figure 4. $C_{61}H_2$: Variation of the atom-localized charges in (a) the 5,6- and (b) the 6,6-isomer as a function of the distance from the C_m atom (see text). Filled squares, $Q_v - 4$; empty squares, $Q_v - Q_{v,d}$.

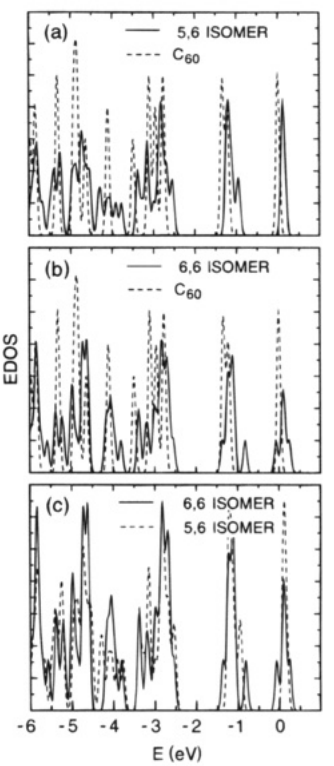

Figure 5. $C_{61}H_2$: Density of the occupied electron states. $E = 0$ corresponds to the position of the HOMO level in C_{60}.

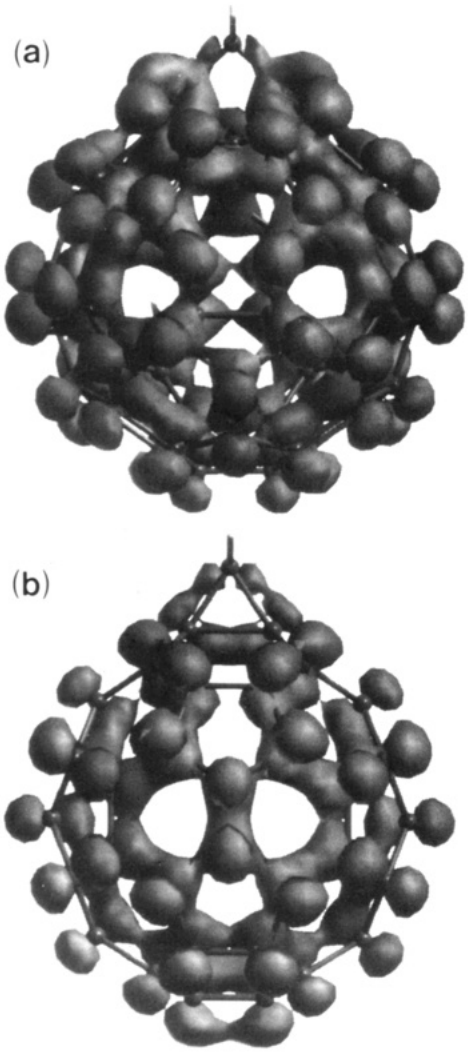

Figure 6. $C_{61}H_2$: Probability isodensity surface (0.03 e/(au)^3) of the fivefold HOMO multiplet in (a) A and (b) B.

is clear in both cases. However, at least in the region plotted (a range of a few electronvolts below the HOMO level), the EDOS is affected to a greater extent in isomer B, consistent with the fact that the partial loss of the double-bond character at the hexagon−hexagon link induces a stronger perturbation in the π system.

Parts a and b of Figure 6 contain a 3D plot of one isodensity surface of the h_{1u}-derived fivefold multiplet for A and B, respectively. A few characteristics can be clearly seen. These orbitals have π-character and are bonding on the bulky fullerene, just as in C_{60}. However, here they also participate in the bonding of the methylene carbon. The orbital deformation induced by the addition of the CH_2 group is strongly localized. This is especially evident in isomer A Figure 6a.

The HOMO−LUMO gap decreases by less than 0.2 eV in both cases. Above the LUMO t_{1u} triplet, the sequence of levels in C_{60} proceeds in two triplets of symmetry t_{1g} and t_{2g}, respectively. In $C_{61}H_2$, admixture of new states localized on the methylene group starts beyond the t_{1g}-derived levels. In B, a new state with large amplitude on CH_2 is well recognizable between the two split triplets. The calculated values of the dipole moment matrix elements for transitions from the h_{1u}-derived states in both isomers, however, show minor changes with respect to the C_{60}. In particular, transitions to the LUMO t_{1u}-derived triplet remain dipole "forbidden", because, in spite of the symmetry lowering, the change in the character of the orbitals is not sufficient to result in a nonnegligible value of the matrix elements. In B the oscillator strength corresponding to the t_{1g}-derived states—the first dipole allowed in C_{60}—keeps the same value, whereas in A it decreases by a factor of ~1.5.

TABLE 5: $C_{61}H_2$. Interatomic Distances (in Å) between Atoms on One Molecule (C, H, C_m) and Those on Nearest-Neighbor Molecules (C*)[a]

isomer	C−C*	C_m−C*	H−C*
A	3.18	3.95	H_1: 2.92, 3.20
			H_2: 3.11, 3.165
B	3.08	3.855	2.78, 3.315, 3.315

[a] Note that in C_{60}, the closest C−C* distance is 3.09 Å.

This discussion is, however, based on an oversimplified one-electron picture and on Kohn−Sham energy levels. It is well-known that in C_{60} the HOMO−LUMO gap is underestimated by ~1 eV in LDA and that excitonic effects dominate the UV absorption spectrum. Here, the scenario will certainly be similar, given that the nature of the electron states is the same as in C_{60}. Also, in our results, "new" empty one-electron states are present at lower energies in the 6,6-isomer. This is consistent with the experimental findings of a new and characteristic feature in the UV spectrum at ~3 eV in the 6,6-isomer.[8] Many-body calculations of the excited molecular states are required to establish the relevance of these findings.

Symmetry lowering with respect to C_{60} is also responsible for the existence of permanent dipole moments in $C_{61}H_2$ along the line joining the methylene carbon to the center of the 60-atom cage. The LDA values are 2.7 D in A and 3.2 D in B. We note that similar values have already been calculated for other molecules derived by doping C_{60}, namely, for $C_{59}B$[34] and for La@C_{60}.[35]

IV. Solids: Solid-State Effects and Comparison of the Two Isomers

Only the crystal structure of the 5,6-annulene isomer has been measured experimentally.[9] It is fcc over 290 K, with the molecules orientationally disordered but with the methyl groups preferentially pointing toward octahedral voids. The lattice constant is 14.19 ± 0.02 Å at 308 K. In our model, the molecules have their centers at the corners of a fcc lattice and are orientationally ordered in such a way that the axis joining the methylene carbon to the center of the bulky fullerene is aligned with the empty octahedral void. For the 6,6-cyclopropane isomer, we have also assumed fcc periodic boundary conditions, with the methylene carbon pointing to the octahedral position. This corresponds to the orientation commonly adopted for band-structure calculations of C_{60}, namely, with double bonds facing the octahedral site. For the sake of comparison also with the C_{60} solid, we have used the same value for the lattice constant of the three compounds (14.1 Å). Note that, however, in contrast with C_{60}, in the $C_{61}H_2$ solids the symmetry is not cubic. In Table 5, we report some of the intermolecular distances, which are significantly different in the two cases. In B, each hydrogen has three carbons as nearest neighbors (1 + 2) on the other molecule, which form two single bonds. In A, all the distances are different, and the three carbons form one single and one double bond. For the C_m atom, we report only the closest distance to the atoms of the neighboring molecules, which in both cases is ~0.8 Å larger than that between the fullerene-type atoms.

We have relaxed the molecular structure in the solid. The effects on the values of the bond lengths and angles are negligible, analogous to our results for C_{60}.[30] The refined values[9] for the radius of the methylene carbon (4.9 ± 0.2 Å) and for that of the carbon shell (3.555 ± 0.007 Å) in the A

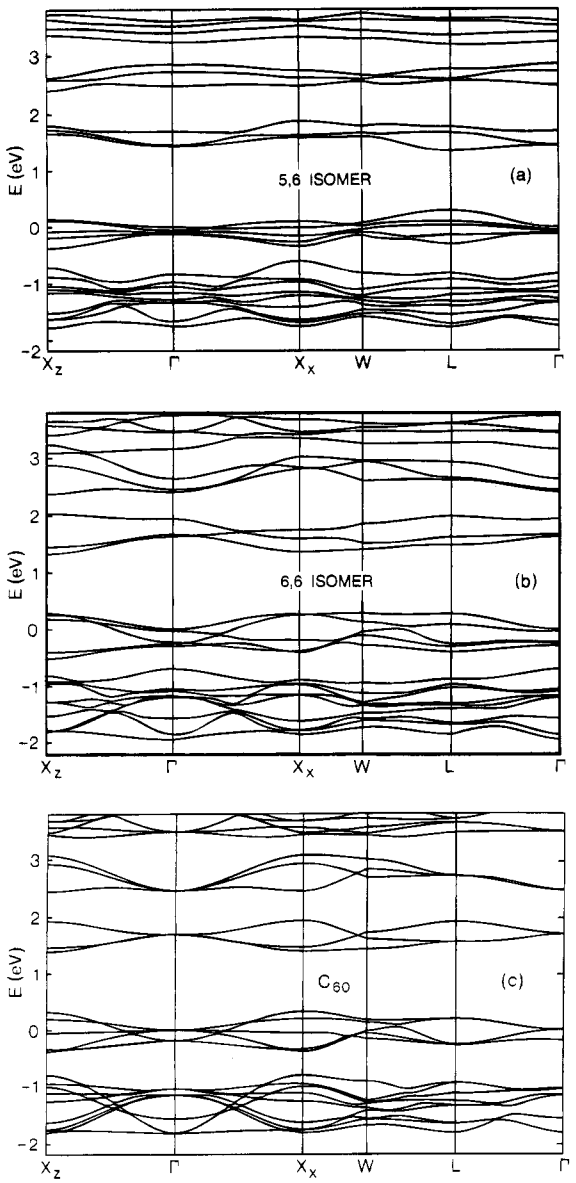

Figure 7. $C_{61}H_2$: Electron energy bands of (a) isomer A, (b) isomer B, and (c) C_{60}. $E = 0$ corresponds to the top of the valence band at Γ in each case.

solid are very close to those of our model (see above).[36] Within the accuracy of the calculations, also the energy difference between the two isomers is unaltered with respect to that of the isolated molecules. Furthermore, calculations on the A solid show that the energy is largely insensitive to the orientation of the molecule in the unit cell. This finding mirrors our results for C_{60} and is consistent with the observation of easy molecular reorientation in the fcc solid in both cases.

The electronic Kohn–Sham energy bands are illustrated in Figure 7a,b over a range of 5 eV around the gap region. Table 6 contains some characteristic features at the edges of the Brillouin zone. While the bands largely resemble broadened molecular levels like in the pure fullerites,[37] the changes with respect to C_{60} (Figure 7c) are not at all negligible. Aside from the splittings stemming from the loss of symmetry, we observe a quite general flattening in A and more complex behavior in B, where, in particular, the "new" molecular state above the t_{1g}-derived triplet broadens and overlaps with the neighboring bands.

Both A and B preserve the character of direct gap semiconductors. However, the fundamental gap moves from X in C_{60} to L in A. Isomer B is a somewhat more unusual case, since, owing to the flattening of the HOMO band, the HOMO-LUMO gaps at different k-points are the same within 0.01 eV.

TABLE 6: $C_{61}H_2$. Some Characteristics of the Kohn–Sham Energy Bands (in eV) in Isomers A and B Compared to C_{60}[a]

compound	$E_g(\Gamma)$	$E_g(X)$	$E_g(L)$	$W(\Gamma)$	$W(X)$	$W(L)$
fcc-C_{60}	1.70	1.07	1.37	0	0.54	0.35
$C_{61}H_2$ (A)	1.44	1.53 (X_z), 1.49	1.05	0.26	0.14 (X_z), 0.28	0.43
$C_{61}H_2$ (B)	1.63	1.04 (X_z), 1.10	1.21	0.32	0.70 (X_z), 0.38	0.50

[a] E_g refers to the HOMO–LUMO gaps, W to the splittings of the t_{1u}-derived states.

Owing to the presence of the CH_2 group along the (001) direction, the energy bands exhibit anisotropy, especially along the Δ-lines connecting Γ to X_z = (001) or X_x = (100). The anisotropy is sizable, especially in isomer B, probably owing to the closer approach of the methylene group of one molecule to the other molecules (see Table 6) and to the higher symmetry. However, in the real material the orientational disorder will tend to mask these effects.

V. Conclusions

We have presented an *ab initio* study of $C_{61}H_2$ based on density functional theory. Depending on whether the methylene group bridges a single or a double bond of C_{60}, two molecular configurations are possible, the former corresponding to bond breaking. The main effects of the CH_2 addition on C_{60} and the distinctive features of the two isomers can be summarized as follows:

(i) Both the structural relaxation and the charge inhomogeneity on the carbon shell are spatially localized.

(ii) The charge transfer to the methylene group is estimated to be less than one electron in both cases.

(iii) The structural distortion is more important and energetically more costly in the 5,6-isomer.

(iv) In both cases, the nature of the electron states lying within a few electronvolts below and above the HOMO is very similar to that of C_{60}. The modifications are localized on the close environment of the two bridging atoms. A new low-energy empty state with large amplitude on the CH_2 group is detected only in the 6,6-isomer.

(v) Significant differences exist in the band structure of the two solids in the region around the fundamental gap.

Experimentally, both isomers have been isolated, and no record exists that interconversion from one to the other has been observed. In the crystalline form, only the 5,6-isomer is so far available. The calculated binding energy difference is too small to account for the preference of one or the other, independent of whether we calculate it in LDA or GCXC. It is reasonable to expect that kinetic effects play a decisive role in determining the relative stability of the two isomers. However, we also note that a lower thermal stability and a higher reactivity can be expected for the 6,6-isomer, consistent with the well-known low stability of cyclopropane molecular derivatives. This could be a possible, nonnegligible distinctive factor for the synthesis of the two solids.

With regard to the physical properties of the solid phases, we can expect some interesting features. The large molecular dipoles may be responsible for materials with unusual dielectric properties. In addition, flattening of the t_{1u}-derived bands with respect to C_{60}, especially in the 5,6-modification, may become of special interest in compounds intercalated with electron donors such as alkali metals. In fact, the enhancement of the density of states at the Fermi energy in the case of partial

occupation of the C_{60} LUMO's is one of the factors that could increase the superconducting transition temperature.

The detailed determination of the electronic and structural properties we presented here can be considered as paradigm for the study of the chemistry of the fulleroids (homofullerenes) as well as that of bridged methanofullerenes, of which $C_{61}H_2$ is the parent. The next step in this research will be the investigation of the dynamics of interconversion.

Acknowledgment. We are particularly indebted to J. E. Fischer, P. A. Heiney, and A. Smith for useful discussions and their critical reading of the manuscript. We also thank the following people for several stimulating discussions: L. Cristofolini, M. Maggini, M. Prato, M. Riccó, C. Thilgen, and F. Wudl.

References and Notes

(1) Taylor, R. In *The Fullerenes*; Kroto, H. W., Walton, D. R. M., Eds.; Cambridge University Press: Cambridge, 1993; pp 87−101.

(2) Hirsch, A. *The Chemistry of Fullerenes*; G. Thieme: Stuttgart, Germany, 1994.

(3) Taylor, R.; Walton, D. R. M. *Nature* **1993**, *363*, 685.

(4) Isaac, L.; Wehrsig, A.; Diederich, F. *Helv. Chim. Acta* **1994**, *76*, 1231. Isaac, L.; Diederich, F. N. *Angew. Chem.*, in press.

(5) Maggini, M.; Scorrano, G.; Prato, M. *J. Am. Chem. Soc.* **1993**, *115*, 9798.

(6) Wudl, F. *Acc. Chem. Res.* **1992**, *25*, 157.

(7) Suzuki, T.; Li, Q.; Khemani, K. C.; Wudl, F. *J. Am. Chem. Soc.* **1992**, *114*, 7301.

(8) Smith, A. B., III; Strongin, R. M.; Brard, L.; Furst, G. T.; Romanow, W. J.; Owens, K. G.; King, R. C. *J. Am. Chem. Soc.* **1993**, *115*, 5829.

(9) Lommen, A.; Heiney, P. A.; Vaughan, G. B. M.; Strongin, R. M.; Brard, L.; Smith, A. B., III; Stephens, P. W.; Liu, D.; Wudl, F.; Suzuki, T.; Li, C.; Khemani, K. C. *Phys. Rev. B* **1994**, *49*, 12572.

(10) Riccó, M.; Cristofolini, L.; Viola, G.; Dalcanale, E. *J. Chem. Phys. Solids* **1993**, *53*, 1487.

(11) Smith, A., private communication.

(12) Fischer, J. E., private communication.

(13) Diederich, F. N.; Isaacs, L.; Philp, D. *J. Chem. Soc. Perkin Trans.* **1994**, *2*, 391 and references therein.

(14) Raghavachari, K.; Sosa, C. *Chem. Phys. Lett.* **1993**, *209*, 223.

(15) Car, R.; Parrinello, M. *Phys. Rev. Lett.* **1985**, *55*, 2471.

(16) Andreoni, W. In *Physics and Chemistry of Fullerenes*; Prassides, K., Ed.; Kluwer Academic: Dordrecht, 1994; pp 169−182.

(17) Kohn, W.; Vashishta, P. In *Theory of the Inhomogeneous Electron Gas*; Lundqvist, S., March, N. H., Eds.; Plenum: New York, 1983; pp 79−147.

(18) Hutter, J.; Lüthi, H. P.; Parrinello, M. *Comp. Mat. Sci.* **1994**, *2*, 244.

(19) Pulay, P. *Chem. Phys. Lett.* **1980**, *73*, 393.

(20) Fischer, T. H.; Almlöf, J. *J. Phys. Chem.* **1992**, *96*, 9768.

(21) Perdew, J. P.; Zunger, A. *Phys. Rev. B* **1981**, *23*, 5048.

(22) Becke, A. *Phys. Rev. A* **1988**, *38*, 3098.

(23) Perdew, J. P. *Phys. Rev. B* **1986**, *33*, 8822; erratum **1986**, *34*, 7406.

(24) Andreoni, W.; Scharf, D.; Giannozzi, P. *Chem. Phys. Lett.* **1990**, *173*, 499.

(25) Troullier, N.; Martins, J. L. *Phys. Rev. B* **1991**, *43*, 1993.

(26) Yannoni, C. S.; Bernier, P. P.; Bethune, D. S.; Meijer, G.; Salem, J. R. *J. Am. Chem. Soc.* **1991**, *113*, 3190.

(27) Röthlisberger, U.; Klein, M. L. *Chem. Phys. Lett.*, in press; *J. Am. Chem. Soc.*, in press.

(28) Johnson, B. G.; Gill, P. M. W.; Pople, J. A. *J. Chem. Phys.* **1993**, *98*, 5612.

(29) Troullier, N.; Martins, J. L. *Phys. Rev. B* **1992**, *46*, 1754.

(30) Andreoni, W.; Giannozzi, P.; Parrinello, M. *Phys. Rev. B*, in press.

(31) Chapuisat, X.; Jean, Y. *Top. Curr. Chem.* **1976**, *68*, 1.

(32) Yamaguchi, Y.; Schaefer, H. F., III; Baldwin, J. E. *Chem. Phys. Lett.* **1991**, *185*, 153.

(33) Ashcroft, N. W.; Mermin, N. D. *Solid State Physics*; Holt, Rinehart and Winston: New York, 1976; p 73.

(34) Andreoni, W.; Gygi, F.; Parrinello, M. *Chem. Phys. Lett.* **1992**, *189*, 241.

(35) Andreoni, W. *Nanostruct. Mater.* **1993**, *3*, 293.

(36) We note that the value *assumed* in ref 9 for the interatomic distance at the bridge is 1.455 Å. This would be consistent with the existence of a real carbon−carbon bond, while at the bridge the bond is broken.

(37) Weaver, J. H.; Poirier, D. M. Solid State Properties of Fullerenes and Fullerene-Based Materials. In *Solid State Physics*; Ehrenreich, H., Spaepen, F., Eds.; Academic Press: New York, 1994; Vol. 48, Chapter 1, pp 1−108.

JP942533Y